Inorganic Chemistry
Article

Inorg. Chem. **2010**, *49*, 3051–3056 **3051**
DOI: 10.1021/ic100100a

Large Changes in Electronic Structures of Ru_2^{6+} Species Caused by the Variations of the Bite Angle of Guanidinate Ligands: Tuning Magnetic Behavior

Gina M. Chiarella, F. Albert Cotton,† Carlos A. Murillo,* Mark D. Young, and Qinliang Zhao

Department of Chemistry, P.O. Box 3012, Texas A&M University, College Station, Texas 77842-3012.
†Deceased, February 20, 2007

Received January 17, 2010

Syntheses and characterization of two Ru_2^{6+} paddlewheel compounds having very different magnetic behavior are reported. The compounds $Ru_2(tbn)_4Cl_2$, **1**, and $Ru_2(tbo)_4Cl_2$, **2** (where tbn = the anion of 1,5,7-triazabicyclo-[4.3.0]non-6-ene and tbo = the anion of 1,4,6-triazabicyclo[3.3.0]oct-4-ene), have four equatorial bicyclic guanidinate ligands and two chloride ions in axial positions. They show large disparity in Ru−Ru distances of about 0.11 Å (2.389(3) and 2.499(3) Å at 30 K for **1** and **2**, respectively) that is attributed to the divergence in the bite angle of the ligand. Variable temperature structural data show no significant changes in the Ru−Ru distances between 30 and 213 K suggesting that the electronic structure remains unchanged in this temperature range for both compounds. Magnetic studies of **1** indicate there are two unpaired electrons at room temperature but the compound behaves as essentially diamagnetic at ∼2 K. Compound **2** is non-magnetic across all temperatures in the range of 2 to 300 K. Density functional theory calculations suggest a $\pi^4\pi^{*4}\delta^2$ electronic configuration for **2**, while the magnetic behavior and structural data for **1** are consistent with a $\sigma^2\pi^4\delta^2\pi^{*2}$ electronic configuration. This shows the importance of the ligand bite angle in determining the electronic configuration of the diruthenium unit and a way to tune magnetic behavior.

Introduction

Since 1964 when the first species containing a direct and unsupported quadruple bond between metal atoms, $Re_2Cl_8^{2-}$, was reported considerable efforts has been focused on the determination of the electronic configuration as a means of explaining various properties in compounds with metal-to-metal bonds.[1] The "traditional" energy ordering of the orbitals of $\sigma < \pi < \delta < \delta^* < \pi^* < \sigma^*$ has been surprisingly useful especially for compounds containing eight or less bonding electrons. However, for species with more than eight electrons this arrangement only serves as a first approximation because in some cases the energy of the antibonding orbitals may be very similar.[1] Early examples are those of compounds containing Ru_2^{n+} cores (n = 4, 5, or 6), in which the δ^* and π^* orbitals are often nearly degenerate,[2,3] leading to variety of electronic structures that are manifested in variations of the metal-to-metal distances[3,4] and magnetism.[5]

It is not often straightforward to separate the effect on the Ru−Ru distances caused by axial ligands or by the nature of the ligands and other variables. However, the effect of the ligands has been relatively well addressed in Ru_2^{6+} compounds.[6−8] More recently theoretical calculations have shed some light on Ru_2^{5+} compounds.[9] In most compounds with Ru_2^{6+} units, which have 10 metal-based electrons, the electronic configuration is $\sigma^2\pi^4\delta^2\delta^{*2}$.[3] However, when strong σ donors, such as cyanide and alkynyl ligands are in axial positions, a significant lengthening of 0.2−0.3 Å in the Ru−Ru bond distances is observed relative to those having weaker σ donor ligands such as Cl. For example, the Ru−Ru bond distances in compounds of the type Ru_2(amidinate)$_4Cl_2$ are generally around 2.30−2.34 Å[3,7] while those

*To whom correspondence should be addressed. E-mail: murillo@tamu.edu.

(1) *Multiple Bonds between Metal Atoms*; Cotton, F. A., Murillo, C. A., Walton, R. A., Eds.; Springer Science and Business Media, Inc.: New York, 2005.
(2) Norman, J. G.; Renzoni, G. E.; Case, D. A. *J. Am. Chem. Soc.* **1979**, *101*, 5256.
(3) Angaridis, P. In *Multiple Bonds between Metal Atoms*; Cotton, F. A., Murillo, C. A., Walton, R. A., Eds.; Springer Science and Business Media, Inc.: New York, 2005; Chapter 9.
(4) Aquino, M. A. S. *Coord. Chem. Rev.* **2004**, *248*, 1025.
(5) See for example: (a) Telser, J.; Drago, R. S. *Inorg. Chem.* **1984**, *23*, 3114. (b) Cukiernik, F. D.; Luneau, D.; Marchon, J.-C.; Maldavi, P. *Inorg. Chem.* **1998**, *37*, 3698. (c) Jiménez-Aparicio, R.; Urbanos, F. A.; Arrieta, J. M. *Inorg. Chem.* **2001**, *40*, 613. (d) Handa, M.; Sayama, Y.; Mikuriya, M.; Nukuda, R.; Hiromitsu, I.; Kasuga, K. *Bull. Chem. Soc. Jpn.* **1995**, *68*, 1647. (e) Cheng, W.-Z.; Cotton, F. A.; Dalal, N. S.; Murillo, C. A.; Ramsey, C. M.; Ren, T.; Wang, X. *J. Am. Chem. Soc.* **2005**, *127*, 12691. (f) Liao, Y.; Shum, W. W.; Miller, J. S. *J. Am. Chem. Soc.* **2002**, *124*, 9336. (g) Barral, M. C.; Herrero, S.; Jiménez-Aparicio, R.; Torres, M. R.; Urbanos, F. A. *Angew. Chem., Int. Ed.* **2005**, *44*, 305. (h) Barral, M. C.; Gallo, T.; Herrero, S.; Jiménez-Aparicio, R.; Torres, M. R.; Urbanos, F. A. *Chem. Eur. J.* **2007**, *13*, 10088. (i) Miyasaka, H.; Motokawa, N.; Matsunaga, S.; Yamashita, M.; Sugimoto, K.; Mori, T.; Toyota, N.; Dunbar, K. *J. Am. Chem. Soc.* **2010**, *132*, 1532.
(6) Xu, G.-L.; Ren, T. *J. Organomet. Chem.* **2002**, *655*, 239.
(7) Bear, J. L.; Li, Y.; Han, B.; Van Caemelbecke, E.; Kadish, K. M. *Inorg. Chem.* **1997**, *36*, 5449.
(8) Xu, G.-L.; Jablonski, C. G.; Ren, T. *Inorg. Chim. Acta* **2003**, *343*, 387.
(9) Barral, M. C.; Casanova, D.; Herrero, S.; Jiménez-Aparicio, R.; Torres, M. R.; Urbanos, F. A. *Chem. Eur. J.* **2010**, *16*, in print.

Published on Web 02/12/2010

in compounds of the type $Ru_2(amidinate)_4(alkynyl)_2$ are about 2.46−2.57 Å.[3,10] It has been suggested that the strong σ donor ligands interact with the σ bonding orbitals of the ruthenium atoms, destabilizing them to such an extent that the σ bond between the metal atoms no longer forms and thus the ground state configuration has been described as $\pi^4\delta^2\pi^{*4}$. This assignment is based on the lengthening of the metal−metal distance and more recently on density functional theory (DFT) calculations provided in a communication.[11] Less understood has been the effect that the bridging ligands exert on metal-based orbitals. It should be noted that with few exceptions, the majority of Ru_2^{6+} compounds contain bridging *N*,*N*′-donor ligands such as aminopyridinates, formamidinates, and benzamidinates.[7]

Up to now there have been only two Ru_2^{6+} species with guanidinate bridging ligands: $Ru_2(hpp)_4Cl_2$[12,13] and $Ru_2(hpp)_4(CF_3SO_3)_2$[13] (hpp = the anion of 1,3,4,6,7,8-hexahydro-*2H*-pyrimido[1,2-*a*]pyrimidine). These compounds show an interesting magnetic behavior being paramagnetic with an $S = 1$ at ambient temperature but essentially diamagnetic at very low temperature. A question that arose was whether this variation in magnetic behavior was due to a change in electronic configuration as the temperature changed. The ambient temperature behavior with two unpaired electrons was inconsistent with a $\sigma^2\pi^4\delta^2\delta^{*2}$ arrangement and thus favored the $\sigma^2\pi^4\delta^2\pi^{*2}$ configuration indicating that the π^* orbital was lower in energy than the δ^* orbital. The question that the magnetic measurements could not resolve unambiguously was whether the low temperature diamagnetism was due to an electronic configuration such as $\sigma^2\pi^4\delta^2\delta^{*2}$ with no unpaired electrons or to some alternative effect. The answer to this question arose from careful structural measurements done at variable temperature.[13] The premise was that a change in electronic configuration as a result of a transfer of two electrons from a π^* orbital to a δ^* orbital would be accompanied by a measurable decrease in the metal-to-metal distance. The reasoning was that electrons occupying a π^* orbital would destabilize the metal−metal bond more than electrons in δ^* orbitals. This hypothesis has since been shown to be valid for some compounds having Ru_2^{5+} cores.[14] For $Ru_2(hpp)_4Cl_2$ and $Ru_2(hpp)_4(CF_3SO_3)_2$, crystallographic measurements at variable temperature showed that the Ru−Ru distances remained unchanged from 27 to 296 K which suggested that the change in magnetism was unrelated to a change in electronic configuration and therefore it was attributed to a large zero-field splitting (ZFS) which contributed to the electron pairing in an $^1A_{1g}$ ($M_s = 0$) state derived from a $^3A_{2g}$ configuration.[5e,14a,15]

In the present study the effect of the bite angle of the ligands on the Ru−Ru bond and magnetism of paddlewheel Ru_2^{6+} species with $[Ru_2(bicyclic\ guanidinate)_4]^{2+}$ cores has been examined using a guanidinate ligand with two fused 5-membered rings (tbo = the anion of 1,4,6-triaza-bicyclo-[3.3.0]oct-4-ene or 2,3,5,6-tetrahydro-1*H*-imidazo[1,2-*a*]-imidazole) and another one with a 5,6-membered ring (tbn = the anion of 1,5,7-triaza-bicyclo-[4.3.0]non-6-ene or 2,3,5,6,7,8-hexahydroimidazo[1,2-*a*]pyrimididine).[16] These ligands are shown in Scheme 1. These and other analogous guanidinate ligands, which often are used in catalytic processes,[17] have been useful for the preparation of quadruply bonded compounds with very interesting electrochemical,[18,19] electronic, and solubility properties.[20,21] It should be noted that bicyclic guanidinate ligands can stabilize dimetal units and provide them with unique characteristics.[16a] A particularly useful property is the stabilization of species in high oxidation states.[21,22] Furthermore guanidinate ligands can also be used to stabilize a series of mononuclear species, and this type of compounds have become increasingly important in coordination chemistry.[16a,23]

Scheme 1. Line Drawings of the Bicyclic Guanidinate Ligand Precursors: (a) Hhpp, (b) Htbn, and (c) Htbo

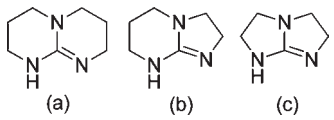

Results and Discussion

Syntheses. Even though the target compounds have Ru_2^{6+} cores, the syntheses were carried out by first reducing $Ru_2(OCCH_3)_4Cl$ with zinc powder in tetrahydrofuran (THF). This somewhat convoluted procedure was necessary because ligand substitution on the easily accessible Ru_2^{5+} species was kinetically too slow to be useful.[24] However, as indicated by an immediate change in the color of the reaction mixture, ligand substitution

(10) Ren, T. *Organometallics* **2005**, *24*, 4854 and references therein.
(11) Liu, I. P.-C.; Ren, T. *Inorg. Chem.* **2009**, *48*, 5608.
(12) Bear, J. L.; Li, Y.; Han, B.; Kadish, K. M. *Inorg. Chem.* **1996**, *35*, 1395.
(13) Cotton, F. A.; Murillo, C. A.; Reibenspies, J. H.; Villagrán, D.; Wang, X.; Wilkinson, C. C. *Inorg. Chem.* **2004**, *43*, 8373.
(14) See for example: (a) Angaridis, P.; Cotton, F. A.; Murillo, C. A.; Villagrán, D.; Wang., W. *J. Am. Chem. Soc.* **2005**, *127*, 5008. (b) Cotton, F. A.; Herrero, S.; Jiménez-Aparicio, R.; Murillo, C. A.; Urbanos, F. A.; Villagrán, D.; Wang, X. *J. Am. Chem. Soc.* **2007**, *129*, 12666 and references therein.
(15) For examples of large ZFS in Ru_2^{n+} species see: (a) Ref 5e. (b) Cotton, F. A.; Miskowski, V. M.; Zhong, B. *J. Am. Chem. Soc.* **1989**, *111*, 6177.
(16) The first name is the von Baeyer name while the second one is the IUPAC name. For a discussion on the nomenclature, see: (a) Coles, M. P. *Chem. Commun.* **2009**, 3659 and references therein. (b) von Baeyer, A. *Ber. Dtsch. Chem. Ges.* **1900**, *33*, 3771. (c) Eckroth, D. R. *J. Org. Chem.* **1967**, *32*, 3362.
(17) Deutsch, J.; Eckelt, R.; Köckritz, A.; Martin, A. *Tetrahedron* **2009**, *65*, 10365.
(18) Cotton, F. A.; Murillo, C. A.; Wang, X.; Wilkinson, C. C. *Inorg. Chem.* **2006**, *45*, 5493.
(19) Cotton, F. A.; Daniels, L. M.; Murillo, C. A.; Timmons, D. J.; Wilkinson, C. C. *J. Am. Chem. Soc.* **2002**, *124*, 9249.
(20) Cotton, F. A.; Murillo, C. A.; Wang, X.; Wilkinson, C. C. *Dalton Trans.* **2007**, 3943.
(21) Cotton, F. A.; Murillo, C. A.; Wang, X.; Wilkinson, C. C. *Dalton Trans.* **2006**, 4623.
(22) See for example: (a) Cotton, F. A.; Gruhn, N. E.; Gu, J.; Huang, P.; Lichtenberger, D. L.; Murillo, C. A.; Van Dorn, L. O.; Wilkinson, C. C. *Science* **2002**, *298*, 1971. (b) Cotton, F. A.; Durivage, J. C.; Gruhn, N. E.; Lichtenberger, D. L.; Murillo, C. A.; Van Dorn, L. O.; Wilkinson, C. C. *J. Chem. Phys. B* **2006**, *110*, 19793.
(23) See for example: (a) Foley, S. R.; Yap, G. P. A.; Richeson, D. S. *Polyhedron* **2002**, *21*, 619. (b) Soria, D. B.; Grundy, J.; Coles, M. P.; Hitchcock, P. B. *J. Organomet. Chem.* **2005**, *690*, 2315. (c) Coles, M. P.; Hitchcock, P. B. *Organometallics* **2003**, *22*, 5201. (d) Coles, M. P.; Hitchcock, P. B. *Dalton Trans.* **2001**, 1169. (e) Coles, M. P.; Hitchcock, P. B. *Inorg. Chim. Acta* **2004**, *357*, 4330. (f) Oakley, S. H.; Coles, M. P.; Hitchcock, P. B. *Inorg. Chem.* **2004**, *43*, 7564. (g) Coles, M. P.; Hitchcock, P. B. *Eur. J. Inorg. Chem.* **2004**, 2662. (h) Irwin, M. D.; Abdou, H. E.; Mohamed, A. A.; Fackler, J. P., Jr. *Chem. Commun.* **2003**, 2882. (i) Feil, F.; Harder, S. *Eur. J. Inorg. Chem.* **2005**, 4438. (j) Wilder, C. B.; Reitfort, L. L.; Abboud, K. A.; McElwee-White, L. *Inorg. Chem.* **2006**, *45*, 263. (k) Rische, D.; Baunemann, A.; Winter, M.; Fischer, R. A. *Inorg. Chem.* **2006**, *45*, 269. (l) Edelmann, F. T. *Chem. Soc. Rev.* **2009**, *38*, 2253.
(24) Whenever we attempted to react overnight $Ru_2(OAc)_4Cl$ with lithium salts of the guanidinates, there was no reaction. From these reaction mixtures, the diruthenium starting material was easily recovered.

was fast upon addition of Li(tbn) or Li(tbo) to THF solutions of $Ru_2(OCCH_3)_4$ prepared in situ by reduction with zinc. The origin of the second Cl axial group is uncertain, but it should be noted that $M_2(hpp)_4$ compounds, M = Mo, W, react with chlorinated solvents to form $M_2(hpp)_4Cl_2$ compounds.[19]

Structural Comparisons. At first glance, the molecular structures of **1** and **2**, shown in Figure 1, are analogous to that of $Ru_2(hpp)_4Cl_2$ having a paddlewheel structure with four equatorially bound guanidinate ligands and two axially coordinated chlorine atoms.[13] However, inspection of the bond distances provided in Table 1 for **1** and **2** show a very large difference in Ru−Ru distances with that for **1** (2.381(2) Å at 213 K) being 0.12 Å shorter than that in **2** (2.5075(16) Å at 213 K). Both of these distances are also longer than that in the hpp analogue (2.3167(6) Å at 213 K). Upon moving from hpp to tbn to tbo, the measured N−C−N angle of the guanidinate ligand increases by approximately 9° for each ligand. The increase in Ru−Ru distance is 0.06 Å between the corresponding hpp and tbn compounds, but doubles to 0.12 Å for the tbn and tbo analogues. This significant increase presumably affects the bonding orbital occupancies (vide infra). It should be noted that the increase in bite angle is not linear with the increase in the bond length between Ru atoms indicating that there is some resistance against lengthening the dimetal unit (vide infra).

For comparison, the Mo−Mo in the quadruply bonded dimolybdenum species with Mo_2^{4+} cores exhibit relatively smaller variations in distances. The distances are 2.067(1) Å for the hpp compound,[19] 2.082(1) Å for the tbn analogue, and 2.1321(7) Å and 2.1453(4) Å for two tbo solvates.[18] These distances increase upon oxidation to Mo_2^{5+} and Mo_2^{6+} species, so that it is 2.240(3) Å in $Mo_2(tbn)_4Cl_2$ and 2.2305(8) Å in $Mo_2(tbo)_4Cl$.[18] An analysis of the idealized metal atom positions, based on the geometry of the tbo ligand in the Mo_2^{4+} species, suggested a Mo−Mo distance of 3.17 Å for $Mo_2(tbo)_4$, instead of the experimental value of 2.13 Å.[18] An analogous analysis for **2**, illustrated in Figure 2, leads to a similar prediction of 3.19 Å for the Ru−Ru bond length, a value that is still longer than the experimental distance of 2.507(2) Å. These compounds clearly show that there is a large impact of the bite angle on the metal−metal distances, but the effect is significantly greater as the bond order decreases.

Finally, it should also be mentioned that the structure of **1** at 30 and 213 K show no appreciable change in bond distances, suggesting that there is only one electronic configuration over the temperature range. Similarly for **2** measurements at 30, 70, and 213 K show no noticeable structural differences. Again, the invariability of the structure is consistent with a sole electronic configuration over the entire temperature range in which measurements were carried out. What is not unambiguous from these measurements is what the electronic configuration is, since the magnetic properties are quite different for the two compounds.

Magnetism. Because compounds with Ru_2^{6+} cores, which have ten electrons occupying the metal-based molecular orbitals, have been characterized with 0, 2, or 4 unpaired electrons,[7] magnetic susceptibility measurements,

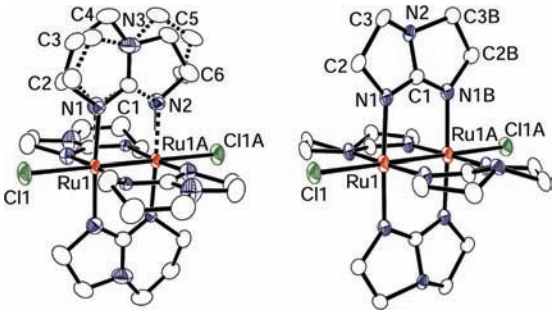

Figure 1. Molecular structures of **1** (left) and **2** (right) drawn with displacement ellipsoids at the 30% probability level. The two orientations of the ligand in **1** (shown only in one of the ligands and omitted in the other three for clarity) are due to the asymmetric rings in the tetragonal space group *I*4/*m*. Note that the ligands are puckered into a boat conformation. Hydrogen atoms are omitted for clarity.

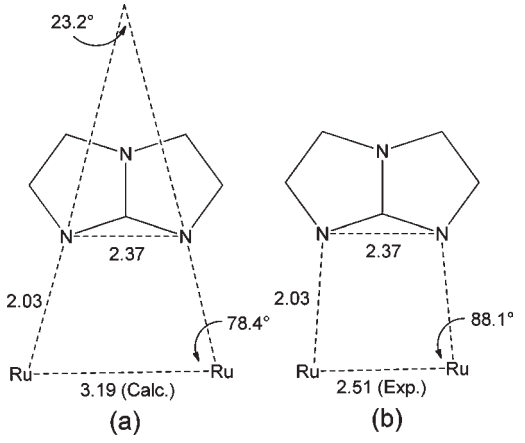

Figure 2. Comparison of (a) the calculated idealized Ru−Ru distance based on the crystal structure geometry of the tbo ligand in **2** to (b) the experimentally observed Ru−Ru distance in **2**. For background on how the estimation of the Ru−Ru distance was done, see ref 18. The schemes are drawn using an arbitrary scale, and the distances are in angstroms.

Table 1. Selected Bond Distances (Å) and Angles (deg) for **1** and **2** at Various Temperatures

	1[a]	**1**[b]	**2**[a]	**2**[c]	**2**[b]
Ru(1)−Ru(1A)	2.381(2)	2.389(3)	2.5075(16)	2.500(3)	2.499(3)
Ru(1)−Cl(1)	2.574(4)	2.570(4)	2.495(3)	2.490(4)	2.489(5)
Ru(1)−N(1)	2.015(14)	1.98(3)	2.032(4)	2.029(6)	2.023(6)
Ru(1A)−N(2)	2.037(19)	1.983(17)			
Cl(1)−Ru(1)−Ru(1A)	180	180	180	180	180
N(1)−Ru(1)−Cl(1)			91.90(9)	91.91(17)	91.81(17)
Ru(1)−Ru(1A)−N(2)	89.6(3)	89.5(5)			
Ru(1A)−Ru(1)−N(1)	89.0(3)	91.2(7)	88.10(9)	88.09(17)	88.19(17)
N(1)−C(1)−N(2)	121.2(8)	126.9(19)	130.9(6)	132.4(10)	130.6(10)

[a] 213 K. [b] 30 K. [c] 70 K.

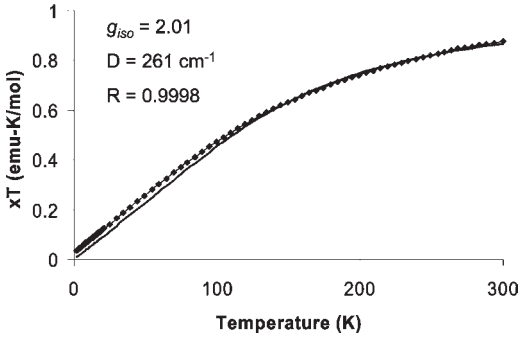

Figure 3. Temperature dependence of the magnetic susceptibility in **1**. The squares represent experimental values, and the solid line is the fitting of these experimental data. The inset shows the fitting parameters. There are two unpaired electrons at ambient temperature but a large ZFS makes the compound appear as essentially diamagnetic at about 2 K.

Table 2. Zero-Field Splitting Parameters for Selected Diruthenium Compounds

compound	D (cm^{-1})	reference
1	261	this work
$Ru_2(hpp)_4Cl_2$	227	13
$Ru_2(hpp)_4(O_3SCF_3)_2$	242	13
$Ru_2(O_2CCH_3)_4$	244	15b
$Ru_2(O_2CC_6H_5)_4(H_2O)_{1.2}(C_2H_5OH)_{0.8}$	215	15b
$[Ru_2(D(3,5\text{-}Cl_2Ph)F)_4Cl(0.5H_2O)]\cdot C_6H_{14}$[a]	79.8	5e

[a] D(3,5-Cl_2Ph)F = the anion of *N*,*N*′-di(3,5-dichlorophenyl)formamidine.

as well as variable temperature structural parameters, are essential to provide insight into the electronic configuration. The room temperature χT value of 0.9 emu·K·mol^{-1} for **1**, shown in Figure 3, is consistent with the presence of two unpaired electrons, as in $Ru_2(hpp)_4Cl_2$.[13] Similarly to $Ru_2(hpp)_4Cl_2$, the magnetism gradually diminishes as the temperature is reduced, and the χT value is essentially zero at 2 K. These magnetic and structural data support an electronic configuration of $\sigma^2\pi^4\delta^2\pi^{*2}$ in which the low temperature diamagnetism may be attributed to a large ZFS. This is further supported by modeling the magnetic data that yields values of $g_{(isO)} = 2.01$, D = 261 cm^{-1}, consistent with earlier work.[7,13] The equation utilized for the magnetic data fitting was

$$\chi = \frac{N\beta^2 g^2}{kT}\cdot\frac{\left[e^{-D/kT} + \left(\frac{2kT}{D}\right)\left(1 - e^{-D/kT}\right)\right]}{\left(1 + 2e^{-D/kT}\right)} \qquad (1)$$

where D is the ZFS parameter, k is the Boltzmann constant, N is Avogadro's number, and β is the Bohr magneton. The ZFS parameter for **1** is the highest yet observed for a Ru_2^{6+} guanidinate compound, but it is consistent with those in other diruthenium compounds, as shown in Table 2.

By contrast **2** is essentially diamagnetic at ambient temperature.[25] The difference in magnetic behavior relative to **1** indicates that the electronic structure must be different and is consistent with the large difference in

(25) For samples of **2**, the values of χT were measured at around 0.1 emu·K·mol^{-1} because of a small amount of a paramagnetic impurity. Unfortunately measurement of the NMR spectrum was precluded by the extreme insolubility of this compound in common organic solvents.

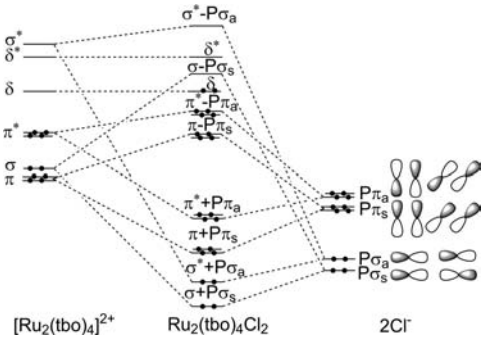

Figure 4. Qualitative molecular orbital energy diagram for **2** (center) and the hypothetical $[Ru_2(tbo)_4]^{2+}$ cation (left).

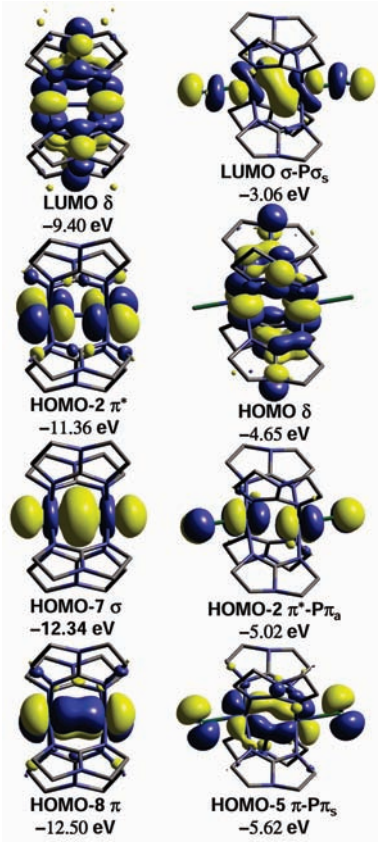

Figure 5. Selected metal-based frontier molecular orbitals for the $[Ru_2(tbo)_4]^{2+}$ model (left) and **2** (right) from DFT calculations.

Ru−Ru distances (vide supra). However, this does not unequivocally answer the question as to what the electronic structure of **2** is.

Computational Studies. DFT calculations were employed to provide a possible explanation of the observed diamagnetism of **2** and offer insight into its electronic structure. Calculations were performed for **2** using the parameters from the crystal structure as a starting geometry and for comparison calculations were also done using the hypothetical cation $[Ru_2(tbo)_4]^{2+}$, which is devoid of axial ligands. The orbital ordering diagram created using the calculations is shown in Figure 4. The calculated energies for the dicationic species indicate that it is the bicyclic guanidinate ligands themselves that mostly destabilize the σ bonding orbital, which becomes higher in energy than the π bonding orbitals.

The antibonding interaction between the metal−metal δ orbital and the P orbitals from the N donor atoms on the guanidinate ligands, as shown in Figure 5, results in the instability of the δ orbital relative to the π^* orbitals. When interactions with the axial chlorine atoms are included in the calculation, the σ bonding orbital is further raised in energy, such that it becomes the lowest unoccupied molecular orbital (LUMO), with an energy above that of the π, π^*, and δ orbitals. Using the results of the calculations, the energies for the π, π^*, δ, and σ orbitals can be assigned as shown in Figure 4. These energies suggest a $\pi^4\pi^{*4}\delta^2$ electronic configuration, and thus a decrease to a formal bond order of one. Because the only net metal−metal bond arises from a δ^2 interaction, the bond is expected to be weak. Thus, the long Ru−Ru bond length in **2** is consistent with this description. It should be noted that this electronic configuration is reminiscent of that of $\pi^4\delta^2\pi^{*4}$ proposed for Ru_2^{6+} compounds having strong σ donating axial ligands.[12−14] Ligands such as −C≡N and −C≡CR interact with the d_{z^2} orbitals of the Ru atoms, raising their energy and also result in a $\pi^4\delta^2\pi^{*4}$ electronic configuration. A recent report by Liu and Ren provided calculations for such molecules.[11] The results showed that the axial acetylide ligands are bent away from the Ru−Ru bond axis in a way that increases the amount of σ and π bonding, explaining the bending observed in such crystal structures. The same type of bending away from the metal−metal bond axis is predicted for the chloride ions in **2**, as seen in Figure 5. However, the prediction is not reflected in the structures of **2**, which shows both chloride ions aligned along the Ru−Ru axis at the three temperatures for which data were collected.

These differences can be accounted for by looking at the Ru−L bonding in the $Ru_2(N-N)_4$ core. Ren describes how the axial bending that increases the Ru−Ru bonding also decreases the Ru−L bonding. Because of the highly divergent nature of the tbo ligand, it is likely that the loss of Ru−L bonding would outpace any gains made from Ru−Ru bonding. In addition, the longer length of the acetylide chains versus that of a single atom species would be expected to make the bending easier.

Conclusions

It has been shown that for Ru_2^{6+} species spanned by four bicyclic guanidinate ligands significant changes in electronic and magnetic properties can be induced by modifications in the ring sizes of the ligands. The electronic structure $Ru_2(tbn)_4Cl_2$ is $\sigma^2\pi^4\delta^2\pi^{*2}$ while that in $Ru_2(tbo)_4Cl_2$ is $\pi^4\pi^{*4}\delta^2$. As a consequence of the changes in configuration, at ambient temperature **1** is paramagnetic while **2** is non-magnetic, consistent with the DFT calculations. The underlying cause of the different electronic configurations is the ligand bite angle. The donor orbitals of the tbo ligand push the ruthenium atoms apart to such an extent that there is a change in the orbital energies, leading to a lower bond order and a significant increase in the metal-to-metal bond distance.

Experimental Section

All syntheses were carried out under inert atmosphere using standard Schlenk techniques unless otherwise noted. The ligand precursors Htbn and Htbo were prepared according to the literature[18] as was $Ru_2(OAc)_4Cl$.[26] Solvents were dried using a Glass Contour solvent system. Mass spectrometry data (electrospray ionization) were recorded at the Laboratory for Biological Mass Spectrometry at Texas A&M University using an MDS Series Qstar Pulsar with a spray voltage of 5 kV. Elemental analyses were performed by Robertson Microlit Laboratories, Inc., Madison, NJ. Infrared spectra were recorded in a Perkin-Elmer 16PC FT-IR spectrophotometer using KBr pellets. Electronic spectra were recorded on a Shimadzu UV-2501 PC spectrophotometer. Variable-temperature magnetic susceptibility measurements were obtained from 2 to 300 K using a Quantum Design SQUID magnetometer MPMS-XL operated at 1000 G. These data were corrected for diamagnetism.

Synthesis of Ru_2(bicyclic guanidinate)$_4Cl_2$, 1 and 2. To a mixture of solid $Ru_2(OAc)_4Cl$ (100 mg, 0.211 mmol) and Zn powder (100 mg, 1.53 mmol) was added 25 mL of THF. The resulting brick red suspension was stirred and gently refluxed overnight. The following morning, the mixture was filtered using a fritted-glass packed with Celite giving a yellow filtrate. To this solution was added 1.0 mmol of the corresponding Li(guanidinate), prepared by adding equimolar amounts of the neutral guanidine and either Bu^{n}Li or MeLi in 25 mL of THF. For each ligand, the solution immediately darkened and was stirred for 30 min. The solvent was then removed under vacuum, and 25 mL of CH_2Cl_2 was added, producing a dark solution (violet-like for **1** and nearly black for **2**). After stirring for 30 min, the solution was exposed to air overnight.

Crystals of **1** were obtained by layering isomeric hexanes onto a CH_2Cl_2 solution of **1**. Yield: 78 mg (48%). Mass spectrum, ESI$^+$: Calcd for M−Cl$^+$: 735 amu. Found: 735 amu. Anal. Calcd[27] for $C_{24}H_{40}N_{12}Cl_2Ru_2$: C, 37.45; H, 5.24%. Found: C, 37.38; H, 5.32%. IR: 2850 (m), 1628 (m), 1542 (s), 1444 (w), and 1264 (m). UV−vis: λ_{max} 535 nm.

Crystals of **2** were obtained by allowing the reaction mixture that had been exposed to air to stand overnight without stirring. Yield: 86 mg (57%). Mass spectrum, ESI$^+$: Calcd for M−Cl$^+$: 679 amu. Found: 679 amu. Anal. Calcd for $C_{20}H_{32}N_{12}Cl_2Ru_2$: C, 33.66; H, 4.52%. Found: C, 33.36; H, 4.25%. IR: 2926 (m), 2852 (m), 1638 (m), 1509 (m), 1440 (w), 1263 (m), 1106 (m) cm^{-1}.

X-ray Structure Determinations. Crystals of **1** and **2** were coated with Paratone oil and mounted on a nylon Cryoloop affixed to a goniometer head. Data for **1** and **2** were collected on a Bruker SMART 1000 CCD area detector system using omega scans of 0.3 deg/frame, with exposures of 30 and 10 s/frame at 30 and 213 K for **1**, 50 s/frames for 30, 70, and 213 K for **2**. Cell parameters were determined using the SMART software suite.[28] Data reduction and integration were performed with the software SAINT.[29] Absorption corrections were applied using the program SADABS.[30] The positions of the Ru atoms were found via direct methods using the program SHELXTL.[31] Subsequent cycles of least-squares refinement followed by difference Fourier

(26) Mitchell, R. W.; Spencer, A.; Wilkinson, G. *J. Chem. Soc., Dalton Trans.* **1973**, 846.

(27) For both $Ru_2(tbn)_4Cl_2$ and $Ru_2(tbo)_4Cl_2$, many attempts were made to obtain an elemental analysis including nitrogen. Without exception, the expected percentages for carbon and hydrogen compositions were satisfactory, but the percentage for nitrogen was slightly low. It should be noted that this is not uncommon for species that produce metal nitrides during combustion.

(28) *SMART for Windows NT*, version 5.618; Bruker Advanced X-ray Solutions, Inc.: Madison, WI, 2001.

(29) *SAINT, Data Reduction Software*, version 6.36A; Bruker Advanced X-ray Solutions, Inc.: Madison, WI, 2001.

(30) *SADABS, Area Detector Absorption and other Corrections Software*, version 2.05; Bruker Advanced X-ray Solutions, Inc.: Madison, WI, 2001.

(31) Sheldrick, G. M. *SHELXTL*, version 6.12; Bruker Advanced X-ray Solutions, Inc.: Madison, WI, 2002.

Table 3. Crystallographic Data for **1** and **2** at Various Temperatures

	1	**1**	**2**	**2**	**2**
chemical formula	$Ru_2C_{24}H_{40}Cl_2N_{12}$	$Ru_2C_{24}H_{40}Cl_2N_{12}$	$Ru_2C_{20}H_{32}Cl_2N_{12}$	$Ru_2C_{20}H_{32}Cl_2N_{12}$	$Ru_2C_{20}H_{32}Cl_2N_{12}$
fw	769.72	769.72	713.62	713.62	713.62
space group	*I*4/*m*	*I*4/*m*	*I*4/*m*	*I*4/*m*	*I*4/*m*
a (Å)	9.608(3)	9.596(3)	8.9365(19)	8.8419(19)	8.827(2)
c (Å)	15.404(7)	15.425(9)	15.349(5)	15.289(4)	15.280(6)
V (Å^3)	1422.1(9)	1420.5(10)	1225.8(5)	1195.3(5)	1190.6(6)
Z	2	2	2	2	2
d_{calcd} (g·cm^{-3})	1.798	1.800	1.933	1.983	1.991
μ (mm^{-1})	1.290	1.291	1.488	1.526	1.532
T (K)	213	30	213	70	30
R1[a] (wR2[b])	0.0680 (0.1483)	0.0696 (0.1145)	0.0393 (0.0865)	0.0557 (0.1301)	0.0536 (0.1247)

[a] $R1 = [\sum w(F_o - F_c)^2/\sum wF_o^2]^{1/2}$. [b] $wR2 = [\sum w(F_o^2 - F_c^2)^2/\sum w(F_o^2)^2]^{1/2}$, $w = 1/[\sigma^2(F_o^2) + (aP)^2 + bP]$, where $P = [\max(F_o^2,0) + 2(F_c^2)]/3$.

syntheses revealed the positions of the remaining non-hydrogen atoms. Hydrogen atoms were added in idealized positions. All hydrogen atoms were included in the calculation of the structure factors. All non-hydrogen atoms were refined with anisotropic displacement parameters. In **1**, the tbn ligands were solved as an average over two orientations, as the asymmetric nature of the ligand rings was disordered over the special position (mirror plane);[32] this structure was refined, following the common practice of choosing the higher symmetry group,[33] in the tetragonal space group *I*4/*m* instead of the non-centric space group $I\bar{4}$ suggested by the SHELXTL program. In **2**, the non-coordinating nitrogen atom from the ligand was disordered and refined over two positions. Data collection and refinement parameters for **1** and **2** are summarized in Table 3. Selected bond distances and angles are listed in Table 1.

Computational Details. DFT[34] calculations were performed with the hybrid Becke's[35] three-parameter exchange functional and the Lee−Yang−Parr[36] non-local correlation functional (B3LYP) in the Gaussian 03 program.[37] Double-ζ quality basis sets (D95)[38] were used on C, N, and H atoms as implemented in Gaussian 03. Correlation consistent double-ζ basis sets (CC-PVDZ)[39] were applied for the Cl atoms. A small effective core potential (ECP) representing the 1s2s2p3s3p3d core was used for the ruthenium atoms along with its corresponding double-ζ basis set (LANL2DZ).[40] All calculations were performed on either Origin 3800 64-processor SGI or Origin 2000 32-processor SGI supercomputers located at the Texas A&M supercomputing facility.

Acknowledgment. This work was supported by the Robert A. Welch Foundation and Texas A&M University. Help with crystallography from Andrey Yakovenko is gratefully acknowledged. The SQUID magnetometer was acquired with a grant from the National Science Foundation (CHE-9974899). C.A.M. also thanks the National Science Foundation for IR/D support.

Supporting Information Available: X-ray crystallographic data in CIF format for **1** and **2**. This material is available free of charge via the Internet at http://pubs.acs.org.

(32) Disorder in paddlewheel compounds with guanidinate ligands is not unusual. See for example: (a) Ref 18. (b) Cotton, F. A.; Murillo, C. A.; Wang, X.; Wilkinson, C. C. *Inorg. Chim. Acta* **2003**, *351*, 191.

(33) Marsh, R. E. *Acta Crystallogr.* **2009**, *B65*, 782.

(34) (a) Hohenberg, P.; Kohn, W. *Phys. Rev.* **1964**, *136*, B864. (b) Parr, R. G.; Yang, W. *Density-Functional Theory of Atoms and Molecules*; Oxford University Press: Oxford, 1989.

(35) (a) Becke, A. D. *Phys. Rev. A* **1988**, *38*, 3098. (b) Becke, A. D. *J. Chem. Phys.* **1993**, *98*, 1372. (c) Becke, A. D. *J. Chem. Phys.* **1993**, *98*, 5648.

(36) Lee, C. T.; Yang, W. T.; Parr, R. G. *Phys. Rev. B* **1998**, *37*, 785.

(37) Frisch, M. J.; Trucks, G. W.; Schlegel, H. B.; Scuseria, G. E.; Robb, M. A.; Cheeseman, J. R.; Montgomery, Jr., J. A.; Vreven, T.; Kudin, K. N.; Burant, J. C.; Millam, J. M.; Iyengar, S. S.; Tomasi, J.; Barone, V.; Mennucci, B.; Cossi, M.; Scalmani, G.; Rega, N.; Petersson, G. A.; Nakatsuji, H.; Hada, M.; Ehara, M.; Toyota, K.; Fukuda, R.; Hasegawa, J.; Ishida, M.; Nakajima, T.; Honda, Y.; Kitao, O.; Nakai, H.; Klene, M.; Li, X.; Knox, J. E.; Hratchian, H. P.; Cross, J. B.; Bakken, V.; Adamo, C.; Jaramillo, J.; Gomperts, R.; Stratmann, R. E.; Yazyev, O.; Austin, A. J.; Cammi, R.; Pomelli, C.; Ochterski, J. W.; Ayala, P. Y.; Morokuma, K.; Voth, G. A.; Salvador, P.; Dannenberg, J. J.; Zakrzewski, V. G.; Dapprich, S.; Daniels, A. D.; Strain, M. C.; Farkas, O.; Malick, D. K.; Rabuck, A. D.; Raghavachari, K.; Foresman, J. B.; Ortiz, J. V.; Cui, Q.; Baboul, A. G.; Clifford, S.; Cioslowski, J.; Stefanov, B. B.; Liu, G.; Liashenko, A.; Piskorz, P.; Komaromi, I.; Martin, R. L.; Fox, D. J.; Keith, T.; Al-Laham, M. A.; Peng, C. Y.; Nanayakkara, A.; Challacombe, M.; Gill, P. M. W.; Johnson, B.; Chen, W.; Wong, M. W.; Gonzalez, C.; Pople, J. A. *Gaussian 03*, Revision C.02; Gaussian, Inc.: Wallingford, CT, 2004

(38) (a) Dunning, T. H.; Hay, P. J. In *Modern Theoretical Chemistry*. *3. Methods of Electronic Structure Theory*; Schaefer, H. F., III, Ed.; Plenum Press: New York, 1977; pp.1−28. (b) Woon, D. E.; Dunning, T. H. *J. Chem. Phys.* **1993**, *98*, 1358.

(39) (a) Dunning, T. H. *J. Chem. Phys.* **1989**, *90*, 1007. (b) Woon, D. E.; Dunning, T. H. *J. Chem. Phys.* **1993**, *98*, 1358. (c) Wilson, A. K.; Woon, D. E.; Peterson, K. A.; Dunning, T. H. *J. Chem. Phys.* **1999**, *110*, 7667.

(40) (a) Wadt, W. R.; Hay, P. J. *J. Chem. Phys.* **1985**, *82*, 284. (b) Hay, P. J.; Wadt, W. R. *J. Chem. Phys.* **1985**, *82*, 299.